

ORIGINAL ARTICLE

Gemcitabine triggers a pro-survival response in pancreatic cancer cells through activation of the MNK2/eIF4E pathway

L Adesso^{1,2}, S Calabretta^{1,2}, F Barbagallo^{1,3}, G Capurso², E Pillozzi², R Geremia¹, G Delle Fave^{1,2} and C Sette^{1,3}

Pancreatic ductal adenocarcinoma (PDAC) is an aggressive neoplastic disease. Gemcitabine, the currently used chemotherapeutic drug for PDAC, elicits only minor benefits, because of the development of escape pathways leading to chemoresistance. Herein, we aimed at investigating the involvement of the mitogen activating protein kinase interacting kinase (MNK)/eIF4E pathway in the acquired drug resistance of PDAC cells. Screening of a cohort of PDAC patients by immunohistochemistry showed that eIF4E phosphorylation correlated with disease grade, early onset of disease and worse prognosis. In PDAC cell lines, chemotherapeutic drugs induced MNK-dependent phosphorylation of eIF4E. Importantly, pharmacological inhibition of MNK activity synergistically enhanced the cytostatic effect of gemcitabine, by promoting apoptosis. RNA interference (RNAi) experiments indicated that MNK2 is mainly responsible for eIF4E phosphorylation and gemcitabine resistance in PDAC cells. Furthermore, we found that gemcitabine induced the expression of the oncogenic splicing factor SRSF1 and splicing of MNK2b, a splice variant that overrides upstream regulatory pathways and confers increased resistance to the drug. Silencing of SRSF1 by RNAi abolished this splicing event and recapitulated the effects of MNK pharmacological or genetic inhibition on eIF4E phosphorylation and apoptosis in gemcitabine-treated cells. Our results highlight a novel pro-survival pathway triggered by gemcitabine in PDAC cells, which leads to MNK2-dependent phosphorylation of eIF4E, suggesting that the MNK/eIF4E pathway represents an escape route utilized by PDAC cells to withstand chemotherapeutic treatments.

Oncogene (2012) **0**, 000–000. doi:10.1038/onc.2012.306

Keywords: eIF4E phosphorylation; MNK2 alternative splicing; drug resistance

INTRODUCTION

Pancreatic ductal adenocarcinoma (PDAC) is a highly malignant neoplastic disease.¹ Gemcitabine, the elective agent used in PDAC chemotherapy, exerts only marginal survival benefits,¹ urging for the identification of new agents and/or therapeutic targets. In this regard, as the PI3K/AKT/mTOR (mammalian target of rapamycin) pathway is activated in approximately half of PDACs, correlating with poor prognosis,² mTOR inhibitors are being considered as possible therapeutic agents in combination with chemotherapy. Nevertheless, their efficacy is often limited by activation of escape pathways leading to phosphorylation of AKT and eIF4E in response to mTOR inhibition.^{3,4} For these reasons, characterization of the molecular mechanisms involved in the acquisition of drug resistance represents a clinical priority.

The mTOR serine/threonine kinase is a central regulator of protein synthesis and cell growth.⁵ mTOR modulates the activity of eIF4E, the core component of the translation initiation complex eIF4F that assembles at the 5' cap of eukaryotic mRNAs.⁵ In quiescent cells, eIF4E activity is restricted by the 4EBPs (eIF4E-binding proteins).^{5–7} Nutrients induce phosphorylation of 4EBPs by mTOR, thereby causing their release from eIF4E and assembly of eIF4F.⁵ Furthermore, eIF4E indirectly stimulates translation by favoring nuclear export of selected mRNAs.⁶ In line with its central role in cell growth, increased eIF4E levels can promote neoplastic transformation.⁷

An additional layer of regulation of eIF4E is provided by its phosphorylation in serine 209 by the mitogen activated protein

kinase (MAPK) interacting kinases (MNK) MNK1 and MNK2,^{8,9} which are activated by ERK1/2 and p38.⁹ Phosphorylation of eIF4E occurs in cells exposed to growth factors and chemotherapeutic agents,^{9,10} and its pharmacological inhibition was shown to reduce proliferation in cancer cells.^{11–13} Importantly, although phosphorylation of eIF4E by MNKs is dispensable for basal protein synthesis and cell viability,⁸ it is essential for the transforming activity of eIF4E in mouse models of cancer,^{14–16} and it positively correlates with poor prognosis and disease grade in human prostate and lung cancers.^{17,18} These observations point to eIF4E phosphorylation as a key step in oncogenic transformation. Noteworthy, as suppression of eIF4E phosphorylation sensitizes cancer cells to growth arrest¹¹ and stress-induced death¹⁹ without affecting normal development or lifespan in animal models,⁸ the MNK/eIF4E pathway appears as a promising pharmacological target for cancer treatment.

Herein, we have investigated the regulation and function of the MNK/eIF4E pathway in PDAC. Phosphorylation of eIF4E positively correlated with grade, and was associated with worse prognosis and earlier disease onset in PDAC patients. MNK2-dependent phosphorylation of eIF4E was induced by gemcitabine in PDAC cells. The drug also promoted upregulation of the splicing factor SRSF1 and splicing of MNK2b, a splice variant that overrides upstream regulatory pathways^{9,20} and confers increased resistance to gemcitabine. Suppression of this pathway by pharmacological or genetic inhibition of either MNKs or SRSF1

¹Department of Biomedicine and Prevention, University of Rome 'Tor Vergata', Rome, Italy; ²Digestive and Liver Disease Unit, II Medical School, University of Rome La Sapienza, Rome, Italy and ³Laboratory of Neuroembryology, Fondazione Santa Lucia, Rome, Italy. Correspondence: Professor G Delle Fave, Digestive and Liver Disease Unit, II Medical School, University of Rome La Sapienza, Rome 00133, Italy or Professor C Sette, Department of Biomedicine and Prevention, University of Rome 'Tor Vergata', Via Montpellier 1, Rome 00133, Italy.

E-mail: gianfranco.dellefave@uniroma1.it or claudio.sette@uniroma2.it

Received 26 December 2011; revised 7 May 2012; accepted 5 June 2012

synergistically enhanced the cytotoxic effects of gemcitabine. Our results highlight a novel pro-survival pathway triggered by gemcitabine in PDAC cells, which leads to MNK2-dependent phosphorylation of eIF4E, suggesting that the MNK/eIF4E pathway might represent a promising therapeutic target for PDAC.

RESULTS

Increased phosphorylation of eIF4E in PDAC correlates with worse prognosis

A cohort of 32 patients diagnosed with primary PDAC in the absence of metastases, who received surgery with radical intent (see Supplementary Table 1), was analyzed for the levels of the phosphorylated form of eIF4E (p-eIF4E) by immunohistochemistry. We found that 27 samples (84.3%) stained positive for p-eIF4E (Figure 1a, Supplementary Table 1). A linear score of staining (range 0–5) was assigned to the samples (Figure 1a; see Materials and methods), and patients were subdivided in two groups: group 0 comprised eight samples displaying no staining (score 0) or low p-eIF4E staining (that is, ≤ 2), whereas group 1 comprised 24 samples displaying strong p-eIF4E staining (that is, ≥ 3) (Figure 1b). The two groups displayed statistically significant differences only for age at diagnosis, grading, progression-free survival and overall survival (Figure 1b). Group 1 patients had a mean age at diagnosis of 64.5, with 95% confidence interval (CI) 59.8–69.2, whereas patients with a low p-eIF4E score (group 0) had a significantly higher mean age at diagnosis of 74.2 (95% CI: 71.9–76.5; $P=0.02$) (Figure 1b). Notably, of the eight patients diagnosed at age ≤ 60 , four had a p-eIF4E score of 5, three had a score of 4 and one a score of 3 (Supplementary Table 1). Furthermore, the p-eIF4E score was positively correlated with tumor grade (G grade, range 1–3; Spearman's coefficient of rank correlation (ρ) = 0.6, $P=0.0008$).

The high p-eIF4E score was also associated with worse survival probability (log-rank test $P=0.02$, Figure 1c). Similarly, in a Cox-proportional hazards regression model, high p-eIF4E score was associated with worse survival (hazard ratio 4.6; 95% CI: 1–20.1). Adjuvant therapy (gemcitabine) was associated with a better overall survival in the Cox-proportional hazards regression model (hazard ratio 0.3; 95% CI: 0.12–0.85), whereas neither the resection margins (R status), nor the lymph node status (N stage or lymph node ratio) were. The mean survival of group 0 patients was 25.1 months (95% CI: 11.3–38.8) as compared with 13 months (95% CI: 8.2–17.8) in group 1 patients ($P=0.04$) (Figure 1b). Elevated p-eIF4E was also associated with shorter 'recurrence-free survival' (log-rank test $P=0.018$). Accordingly, the mean time to tumor recurrence was 20.6 months for group 0 and 9 months for group 1 ($P=0.02$) (Figure 1b). Collectively, these data suggest that eIF4E phosphorylation is directly correlated with tumor grade and associated with worse survival probability.

Therapeutic drugs induce eIF4E phosphorylation in PDAC cells

The marginal survival benefits observed in patients¹ may suggest that chemotherapeutic treatments trigger the activation of pro-survival pathways in PDAC cells. The MNK/eIF4E and the AKT/mTOR pathways are two pro-survival routes frequently activated in cancer.^{3,4} To test whether they contribute to drug resistance in PDAC cells, we analyzed activation of key proteins in these pathways. Phosphorylation of eIF4E was induced by treatment with gemcitabine in several poorly differentiated PDAC cell lines, such as MiaPaCa2 (Figure 2a), PT45P1 (Figure 2b) and PANC-1 cells (Supplementary Figure S1A), as well as in the well-differentiated HPAF2 cells (Supplementary Figure S1A). Activation of the MNK/eIF4E pathway was a specific response, as no increase in AKT phosphorylation occurred under these conditions (data not shown), whereas the decreased phosphorylation of the ribosomal

protein rpS6 indicated that the mTOR pathway was inhibited by gemcitabine (Figures 2a,b).

Next, we tested whether activation of the MNK/eIF4E pathway was triggered by other chemotherapeutic treatments. eIF4E phosphorylation was also increased in response to cisplatin in PDAC cells (Supplementary Figure S1B), whereas neither phosphorylation of AKT (data not shown) nor activation of the mTOR pathway were observed (Supplementary Figure S1B). PDAC cells were also treated with the mTOR inhibitor rapamycin (1 and 10 nM) for up to 24 h. As for other cancer cells,^{3,4} mTOR inhibition caused an increase in phosphorylation of both AKT and eIF4E in PDAC cells (Supplementary Figures S1C, D). However, AKT phosphorylation returned to basal levels by 4–24 h of treatment with the higher dose of rapamycin, whereas eIF4E phosphorylation persisted for the whole duration of the experiment, regardless of the dose used (Supplementary Figures S1C, D). These results suggest that eIF4E phosphorylation is a general, long-lasting feedback response of PDAC cells to therapeutic treatments.

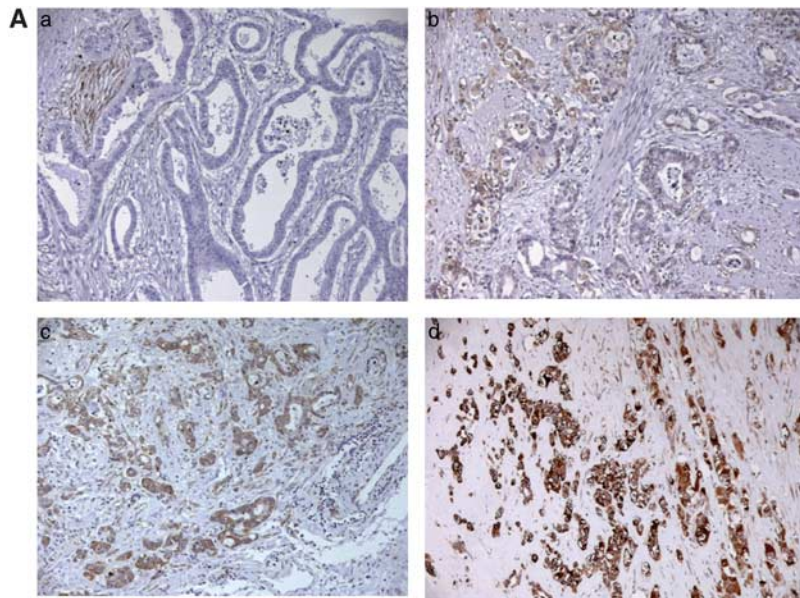
Inhibition of eIF4E phosphorylation enhances the cytostatic effect of therapeutic drugs

To test the most effective tool to interfere with eIF4E phosphorylation in PDAC cells, we treated them with inhibitors of kinases acting upstream of the MAPK/MNK pathway.⁹ The PI3K inhibitor (LY294002), MEK1/2 inhibitor (U0126) and p38 inhibitor (SB202190), alone or in combination, only partially reverted the increased phosphorylation of eIF4E induced by gemcitabine and rapamycin in the poorly differentiated MiaPaCa2 and PT45P1 cell lines (Supplementary Figures S2A, B). However, direct inhibition of MNKs by their chemical inhibitor MNK-I completely abolished eIF4E phosphorylation under all treatments (Supplementary Figure S2A,B). Moreover, MNK-I also strongly reduced gemcitabine-induced eIF4E phosphorylation in the well-differentiated HPAF2 cells (Supplementary Figure S2C). Thus, MNK-I was selected for further studies.

Dose-response experiments showed that MiaPaCa2 cells were highly resistant to gemcitabine, with less than 50% growth inhibition at 100 nM (Supplementary Figure S3A), whereas an almost complete suppression of PT45P1 cell growth was achieved at 30 nM (Supplementary Figure S3B). Thus, to test the effect of MNK-I on PDAC cell growth, we used sub-optimal doses of gemcitabine (30 nM for MiaPaCa2 and 0.1 nM for PT45P1). MNK-I alone slightly reduced growth of both cell lines (Figures 2c, d), to an extent similar to the sub-optimal doses of gemcitabine. However, the combined treatment with the two drugs synergistically inhibited PDAC cell growth, with an almost complete block achieved in PT45P1. A similar synergic effect was also observed in the well-differentiated HPAF2 cells (Supplementary Figure S3C). Furthermore, inhibition of eIF4E phosphorylation by MNK-I significantly augmented the cytostatic effects of cisplatin and rapamycin (Supplementary Figures S3D, E), indicating that activation of this pathway exerts a general positive effect in the stress response of PDAC cells.

Inhibition of MNK activity enhances gemcitabine-induced apoptosis in MiaPaCa2 cells

Clonogenic assays were performed to directly test whether MNK-I enhanced the cytotoxic activity of gemcitabine. MiaPaCa2 cells, which were chosen for their higher resistance to the drug, were cultured for 24 h with sub-optimal doses of gemcitabine (0.1–0.3 nM) with or without MNK-I (10 μ M) and then grown for 10 days in complete medium ($\pm 5 \mu$ M MNK-I). Under these conditions, MNK-I suppressed eIF4E phosphorylation in the large majority of the cells (Supplementary Figure S4A). Gemcitabine reduced the number of colonies in a dose-dependent manner, whereas MNK-I did not significantly affect their number (Figure 3b), even though it reduced the size of colonies



B

| p-eIF4E score | Grading (G1 or G2) n patients | age at diagnosis | survival (months) | time of recurrence (months) | N stage 1 (n patients) | Resection margin (R1) | Adjuvant treatment (n patients) |
|------------------------------------|----------------------------------|------------------|-------------------|-----------------------------|------------------------|-----------------------|---------------------------------|
| GROUP 0 (≤ 2) n=8 | 6 (75%) | 74.2 | 25.1 | 20.6 | 6 (75%) | 3 (37,5%) | 6 (75%) |
| GROUP 1 (>math>\geq 3</math>) n=24 | 5 (20,8%) | 64.5 | 13 | 9 | 17 (70,9%) | 13 (54,2%) | 18 (75%) |
| p value | 0.004 | 0.02 | 0.04 | 0.02 | 1 | 0.4 | 1 |

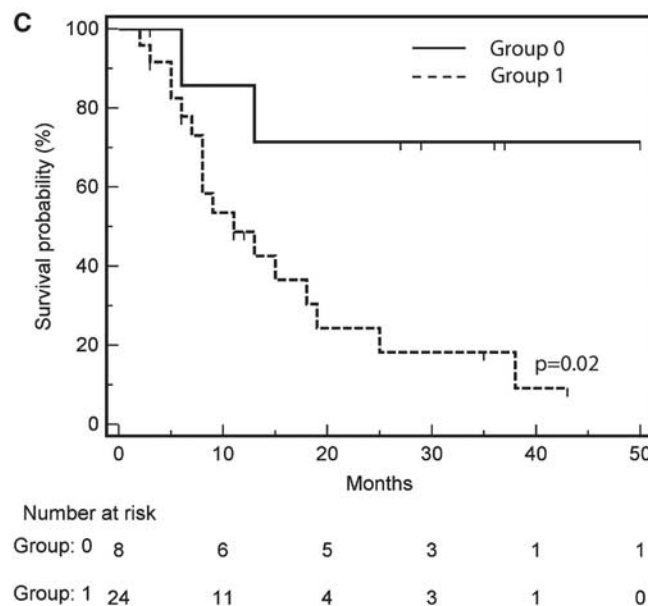


Figure 1. Phosphorylation of eIF4E in PDAC. **(A)** Examples of p-eIF4E immunohistochemistry of PDAC tissues. Panels (a–d) show different intensity of staining. (a) Well-differentiated PDAC with no p-eIF4E staining in the gland and few positive stromal cells (score 0); (b) moderately differentiated (G2) PDAC tissue with mild cytoplasmic staining in few neoplastic glands (score 1); (c) moderately differentiated (G2) PDAC tissue showing cytoplasmic staining in most glands (score 2); (d) poorly differentiated (G3) PDAC tissue with strong cytoplasmic staining (score 3). **(B)** Summary of the clinical-pathological features associated with patients in group 0 (low p-eIF4E) and group 1 (high p-eIF4E). Categorical variables were analyzed by Fisher's test, continuous variables by *t*-test for independent samples. **(C)** Survival likelihood of PDAC patients. Group 0 comprised 8 patients with low p-eIF4E staining (score ≤ 2), group 1 comprised 24 patients with high p-eIF4E (score ≥ 3); $P = 0.02$ at log-rank test. Patients lost at follow-up are 'censored' and marked as small vertical lines.

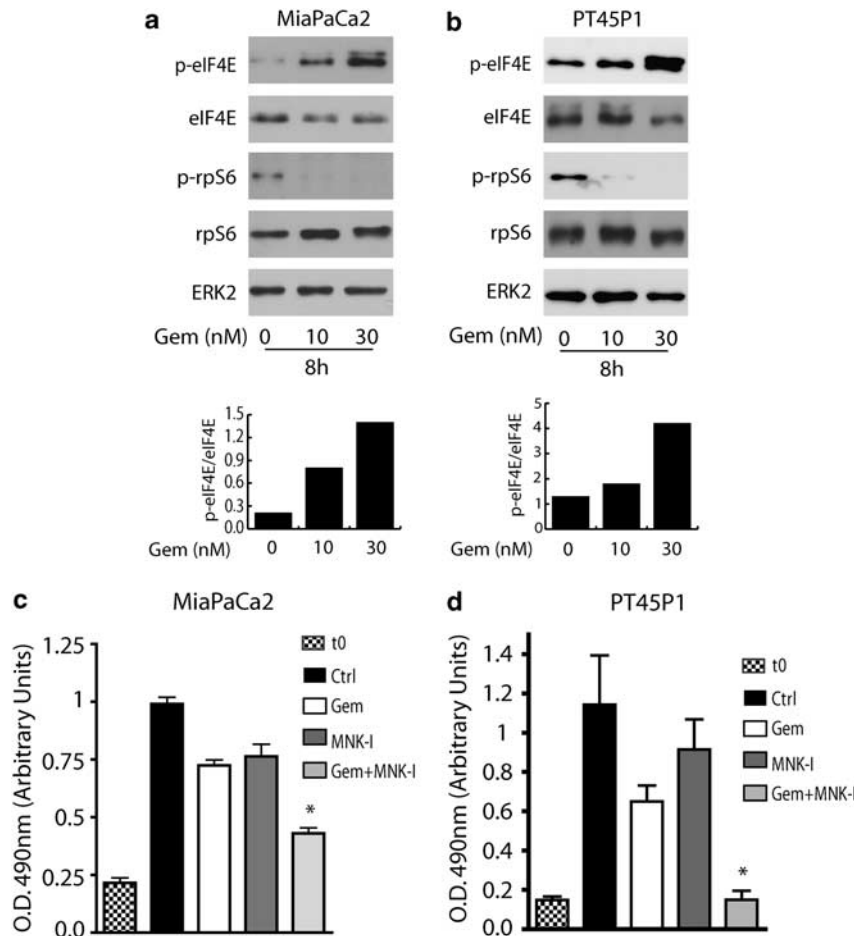


Figure 2. MNK-dependent phosphorylation of eIF4E supports growth of PDAC cells exposed to gemcitabine. Western blot analysis with antibodies for the total or phosphorylated forms of the indicated proteins in MiaPaCa2 (**a**) and PT45P1 (**b**) cells treated for 8 h with 10 and 30 nM gemcitabine. ERK2 was used as loading control. Histograms represent densitometric analysis of p-eIF4E/eIF4E ratio of the gels shown. Viability of MiaPaCa2 (**c**) and PT45P1 (**d**) cell lines was measured by MTS assay after 72 h of exposure to 30 nM gemcitabine alone or in combination with 10 μ M MNK-I. Mean \pm s.d. of three experiments performed in triplicate; * $P < 0.01$ in paired *t*-test.

(Figure 3a). Notably, the combined treatment with the two drugs almost completely suppressed colony formation (Figures 3a, b), confirming a synergic effect.

To understand whether MNK-I affected cell proliferation and/or death, we analyzed cell cycle progression and apoptosis. Treatment of MiaPaCa2 cells with MNK-I and gemcitabine for 72 h caused a slight increase in the percentage of cells in G1 (Supplementary Figure S4B). The combined treatment exerted an additive effect, which was, however, not statistically significant. By contrast, immunofluorescence analysis of the cleaved/activated form of caspase-3 (Figure 3c, Supplementary Figure S4C) and TUNEL assays (Figure 3d, Supplementary Figure S4C) documented that MNK-I significantly increased cell death in cells exposed to gemcitabine, even though it did not trigger apoptosis when it was administered alone (Figures 3c, d). Notably, MNK-I also enhanced the cytotoxic effects of cisplatin in MiaPaCa2 cells (Supplementary Figure S4D). These results suggest that the synergic inhibitory effect on cell growth and colony formation exerted by MNK-I is mainly because of enhanced apoptosis in gemcitabine-treated cells.

MNK2 is required for resistance of MiaPaCa2 cells to gemcitabine. To overcome possible off-target effects of MNK-I, we set out to interfere with MNK1/2 function by other means. MiaPaCa2 cells were transfected with MNK1 and MNK2 siRNAs (small interference

RNAs) and depletion of the mRNAs corresponding to both splice variants was determined by RT-PCR (Figure 4a). Decreased expression of either MNK1 or MNK2 protein (Figure 4b) reduced eIF4E phosphorylation under basal conditions, with MNK2 exerting a stronger effect (Figure 4c). Furthermore, the increased phosphorylation of eIF4E triggered by gemcitabine was completely suppressed after silencing of MNK2, whereas MNK1 depletion only slightly reduced it (Figure 4c). Silencing of MNK2 suppressed gemcitabine-induced eIF4E phosphorylation also in PT45P1 and HPAF2 cells (Supplementary Figure S5A). These results suggest that MNK2 is predominantly responsible for eIF4E phosphorylation in PDAC cells treated with gemcitabine.

Next, MiaPaCa2 cells transfected with si-MNK1 and si-MNK2 were cultured with or without gemcitabine for 48 h. In the absence of the drug, silencing of either MNK1 or MNK2 caused a small reduction of cell growth (15–20%) compared with cells transfected with a control siRNA, whereas concomitant silencing of both MNKs elicited an additive effect (40% inhibition) (Figure 4d). However, in the presence of gemcitabine, which caused a 40% reduction in cell growth *per se* (Figure 4d), the effect of MNK2 depletion was significantly stronger than MNK1 depletion (75% inhibition vs 60% inhibition). Moreover, depletion of both kinases did not significantly increase the effect of MNK2 depletion alone in cells treated with gemcitabine (Figure 4d).

To investigate whether reduced growth was ascribable to increased cell death, as in the case of the MNK-I, we analyzed

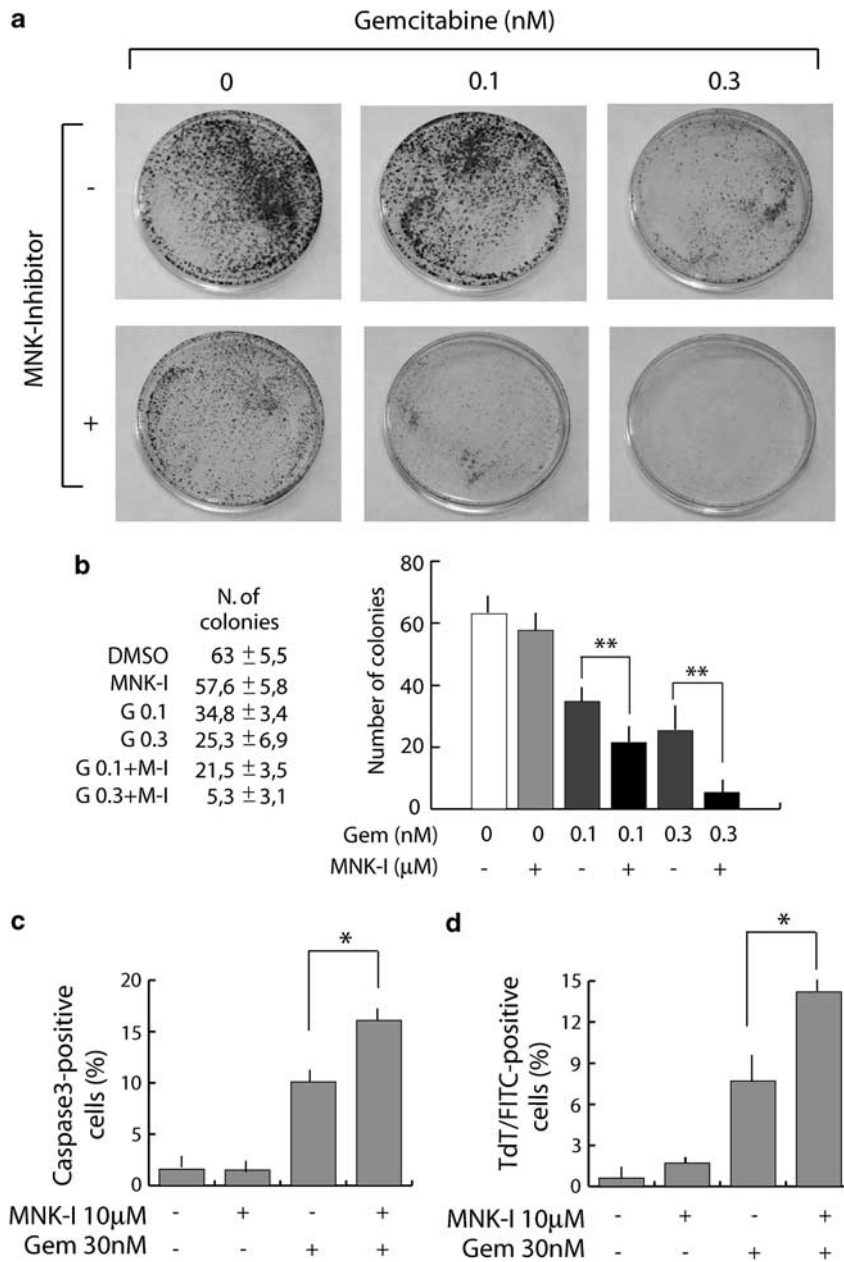


Figure 3. Inhibition of MNK activity enhances the cytotoxic effect of gemcitabine. **(a)** Representative images of colonies of clonogenic assays. **(b)** Histogram shows colony numbers from three experiments (mean \pm s.d.). Actual numbers are reported to the left of the histogram. $**P < 0.005$ in paired *t*-test. **(c, d)** Results of the immunofluorescence analyses of the cleaved form of caspase-3 **(c)** and TUNEL **(d)** in MiaPaCa2 cells treated as indicated. Histograms represent mean \pm s.d. of three experiments; $*P < 0.01$ in paired *t*-test.

apoptosis. We found that silencing of neither MNK1 nor MNK2 affected the viability of control cells (Figure 4e). However, depletion of MNK2, but not MNK1, significantly augmented apoptosis in the presence of gemcitabine (Figure 4e), thus recapitulating the effect of MNK-I. Importantly, similar results were also obtained in PT45P1 and HPAF2 cells (Supplementary Figures S5B, C). These results strongly suggest that MNK2-dependent phosphorylation of eIF4E contributes to the protective response of PDAC cells to gemcitabine.

SRSF1 promotes splicing of the MNK2b variant in gemcitabine-treated MiaPaCa2 cells

On the basis of its prominent role in the response of PDAC cells to gemcitabine, we focused on MNK2. The *MKNK2* gene encodes two

splice variants, named MNK2a and MNK2b.⁹ Notably, the b variant lacks the MAPK-interacting domain,²⁰ which uncouples its activation from this upstream pathway (Figure 5a).^{9,20,21} Treatment with gemcitabine for 48 and 72 h modulated the expression of *MKNK2* in PDAC cells, by causing a reduction in expression of MNK2 (Figure 5b; Supplementary Figure S6A). Concomitantly with the reduction, gemcitabine also altered the ratio between the MNK2 splice variants in favor of MNK2b (Figure 5b; Supplementary Figure S6A). Importantly, we found that expression of recombinant GFP-MNK2b attenuated gemcitabine-dependent cell death in transfected MiaPaCa2 cells, whereas transfection of GFP-MNK2a did not exert any effect (Figure 5c; Supplementary Figure S6B). This result suggests that the shift toward the MNK2b variant in response to the treatment of MiaPaCa2 cells with gemcitabine contributes to reduce their sensitivity to the drug.

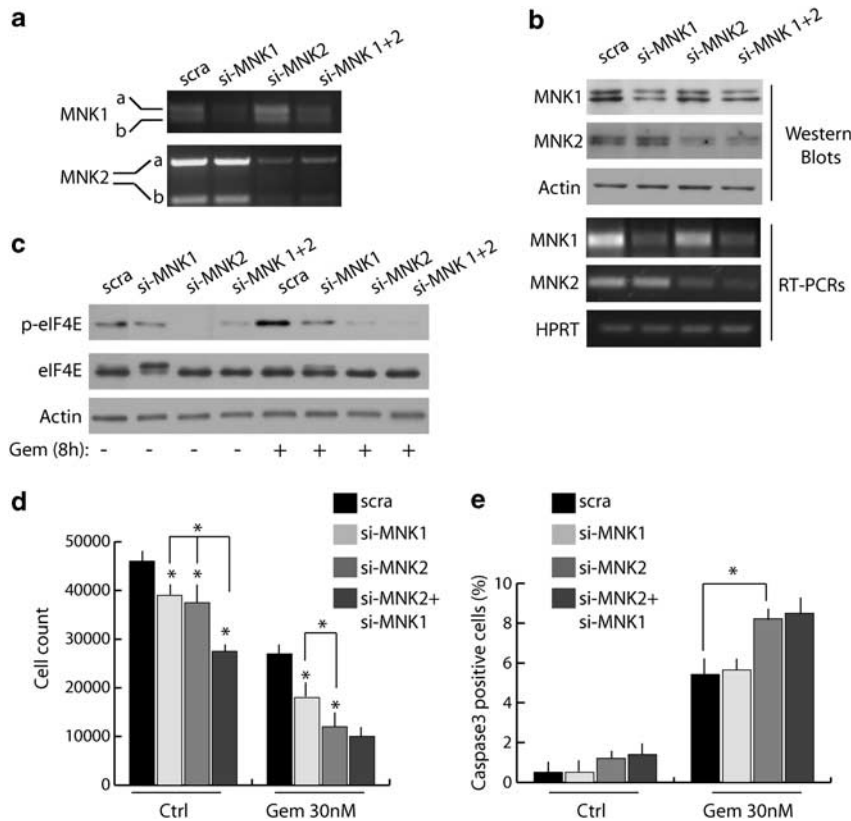


Figure 4. MNK2 promotes eIF4E phosphorylation and survival in gemcitabine-treated cells. **(a)** RT-PCR analysis of the transcripts encoding MNK1 and MNK2 using primers that distinguish between the a and b variants in MiaPaCa2 cells transfected with the indicated siRNAs. **(b)** Western blot and RT-PCR analyses of MNK1 and MNK2 protein and mRNA levels in MiaPaCa2 cells transfected with the indicated siRNAs. First and second panels show protein amounts of MNK1 or MNK2 after transfection. Actin was used as loading control. PCR amplifications were obtained with primers common to both splice variants of MNK1 (fourth panel) and MNK2 (fifth panel). **(c)** Western blot analyses of total and p-eIF4E levels in MiaPaCa2 cells transfected as in **(b)** and treated with or without 30 nM gemcitabine (8 h). **(d–e)** MiaPaCa2 cells transfected as in **(b)** were treated with 30 nM gemcitabine (48 h). The histogram in **(d)** represents cell number of three experiments (mean \pm s.d.). The histogram in **(e)** represents the percentage of cleaved-caspase-3 positive cells of three experiments (mean \pm s.d.). Statistical analysis was performed comparing values of cells silenced for MNKs with cells transfected with the scramble siRNA, or between the samples indicated by brackets; * $P < 0.05$ in paired *t*-test.

In other cell types splicing of MNK2b is promoted by SRSF1, a splicing factor of the SR protein family that functions as a proto-oncogene *in vitro* and *in vivo*.²¹ Remarkably, gemcitabine induced expression of SRSF1 in MiaPaCa2 and PT45P1 cells (Figure 5d). SRSF1 upregulation was specific because other oncogenic splicing factors, such as hnRNPA1²² and Sam68,²³ were not affected (Figure 5d). To investigate the role of SRSF1 in the alternative splicing of MNK2, we silenced it by RNAi. SRSF1 mRNA was decreased already at 24 h from transfection (Supplementary Figure S7), but SRSF1 protein depletion was only observed after 48 h and correlated with increased splicing of the MNK2a variant (Figure 6a). At this time-point, MiaPaCa2 cells were treated with gemcitabine for 48 h and analyzed for MNK2b expression and eIF4E phosphorylation levels. Although SRSF1 silencing did not affect eIF4E phosphorylation in cells growing in control medium (Figures 6a, b), it dramatically reduced it in gemcitabine-treated cells (Figure 6b). Moreover, SRSF1 depletion prevented the gemcitabine-induced shift of variants ratio toward MNK2b (Figure 6b), without affecting the reduction in the total levels of MNK2. These changes in MNK2 splicing and eIF4E phosphorylation were paralleled by reduced proliferation (Figure 6c) and increased death (Figure 6d) in SRSF1-depleted cells exposed to gemcitabine, similarly to what observed by MNK2 silencing and pharmacological inhibition of MNK activity.

Collectively, these observations strongly suggest that upon exposure to gemcitabine, PDAC cells activate a pro-survival

pathway that involves upregulation of SRSF1, splicing of the MNK2b variant and increased phosphorylation of eIF4E.

DISCUSSION

PDAC is a non curable disease, mainly owing to late diagnosis and resistance to therapies, which results in rapid progression and metastatic spreading.¹ In this work, we found that various therapeutic treatments trigger MNK-dependent phosphorylation of eIF4E in PDAC cell models. The biological relevance of this phenomenon is indicated by the enhanced cell death in response to gemcitabine observed in PDAC cells in which eIF4E phosphorylation is prevented by pharmacological or genetic approaches. Furthermore, increased phosphorylation of eIF4E correlates with worse prognosis and disease grade in patients. Thus, these results suggest that the MNK/eIF4E pathway might represent a novel potential therapeutic target for PDAC.

Phosphorylation of eIF4E is associated with worse prognosis in lung cancer,¹⁸ and it is required for the oncogenic properties of eIF4E in animal models.^{14–16} To investigate whether phosphorylation of eIF4E displays clinical relevance in PDAC, we analyzed a cohort of 32 patients selected for the availability of detailed clinical and histopathological data and for the absence of metastases at diagnosis. We found that increased phosphorylation of eIF4E positively correlated with disease grade and was significantly associated with early disease onset in PDAC patients.

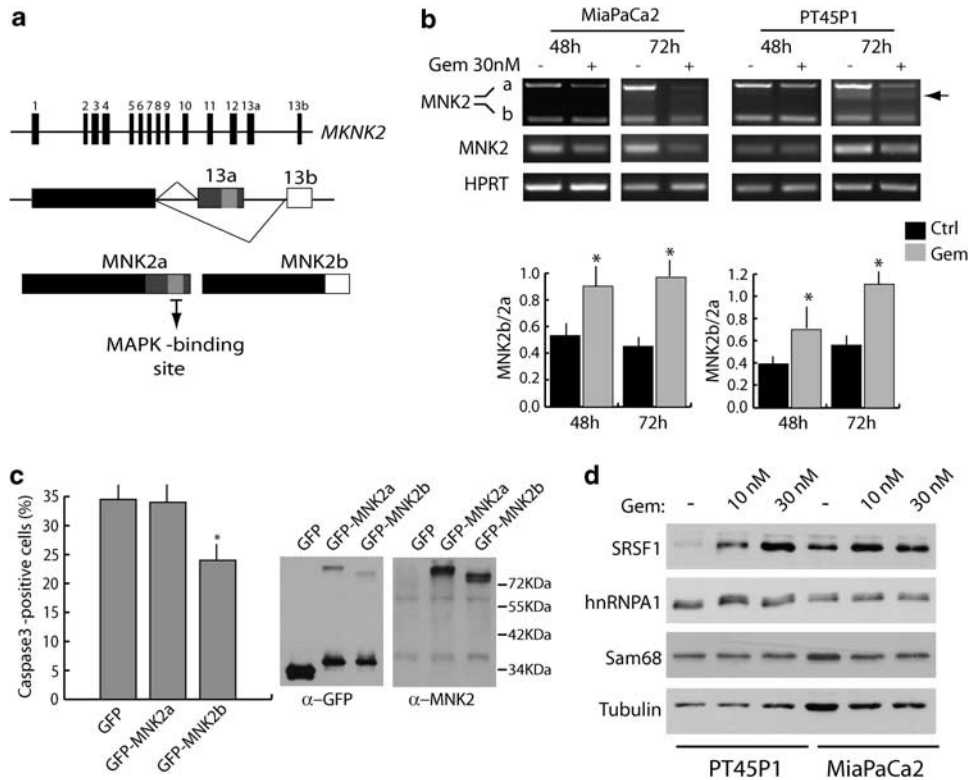


Figure 5. Gemcitabine affects the *MKNK2* splice variants ratio in PDAC cells. **(a)** Schematic representation of the *MKNK2* gene showing the mutually exclusive exons 13a and 13b. **(b)** RT-PCR analysis of MiaPaCa2 or PT45P1 cells treated with 30 nM gemcitabine. Panels show expression of splice variants (the arrow indicates a non specific band appearing with increased PCR cycles in PT45P1), total MNK2 levels and HPRT expression as internal control of the RNA quality. The histograms represent densitometric analysis of the MNK2b/a ratio from three experiments (mean \pm s.d.); * $P < 0.05$ in paired *t*-test. **(c)** Results of the immunofluorescence analyses of the cleaved form of caspase-3 in MiaPaCa2 cells overexpressing GFP, GFP-MNK2a or GFP-MNK2b vectors and treated with gemcitabine for 48 h. Bar graphs represent mean \pm s.d. of three experiments. Statistical analysis was performed using the paired *t*-test; * $P < 0.01$. Right panels represent western blots of the same samples using GFP or MNK2 antibody. **(d)** Western blot analysis of SRSF1, Sam68 and hnRNPA1 in MiaPaCa2 and PT45P1 cells after 72 h of treatment with the indicated doses of gemcitabine.

Furthermore, high eIF4E phosphorylation levels were also associated with worse survival and with a shorter mean time to tumor recurrence. Although the cohort examined in our study was relatively small, our results were statistically significant. However, as some of the patients were also lost to follow-up relatively early, more extensive analyses with larger patient numbers will be required to confirm that eIF4E phosphorylation may represent an important prognostic marker for PDAC. A larger cohort will also be necessary to determine whether increased eIF4E phosphorylation levels reflect an underlying biology associated with earlier onset and more aggressive disease.

Increased phosphorylation of eIF4E occurs in cancer cells of various organs after exposure to stress stimuli and chemotherapeutic treatments,^{9–16} thus suggesting that this pathway allows cells to survive under adaptive pressures. Our results now indicate that MNK-dependent phosphorylation of eIF4E also promotes survival of PDAC cells exposed to therapeutic drugs. Although pharmacological inhibition of MNK activity had mild effects on cell growth, it strongly enhanced the cytostatic effect exerted by genotoxic stress and mTOR inhibition. Our studies indicate that MNK-I mainly affects cell survival in response to gemcitabine. Importantly, sub-optimal doses of gemcitabine combined with MNK-I were sufficient to completely prevent colony formation. As MNK activity and eIF4E phosphorylation are dispensable for normal organism development,⁸ inhibition of this pathway might be well tolerated in combination with other therapeutic treatments. In this regard, it also appears promising the recent observation that inhibition of eIF4E activity by ribavirin exhibited

substantial clinical benefits in acute myeloid leukemia patients without eliciting toxic responses.²⁴ As chemotherapeutic regimens exert only marginal effects in PDAC patients,¹ our findings of the possible role of eIF4E phosphorylation in drug sensitivity of PDAC cells suggest that targeting eIF4E phosphorylation might represent a novel strategy to improve therapeutic efficacy. Notably, this approach might also be useful in combination with other targeted therapies currently under evaluation in PDAC. For instance, RAD001 (Everolimus), a small-molecule mTOR inhibitor derived from rapamycin, exerted positive effects in combination with gemcitabine in preclinical and clinical studies with metastatic PDAC patients.²⁵ However, a side effect of blocking mTOR activity is the increased MNK-dependent phosphorylation of eIF4E.^{3,4} As inhibition of MNK activity synergistically enhances the cytostatic effect of mTOR inhibitors in PDAC cells, it is possible that combined treatment with these molecules might exert beneficial effects.

Phosphorylation of eIF4E promotes tumor development *in vivo*.^{14–16} The activation of MNKs and eIF4E phosphorylation reported in several human cancer cell lines further support the implication of this pathway in oncogenesis.^{11–13} In line with this hypothesis, pharmacological inhibition of MNK activity was shown to reduce protein synthesis,¹¹ cancer cell proliferation^{11–13} and development of tumors *in vivo*.¹² However, all these studies did not document a clear difference between the contribution of MNK1 and MNK2 to these processes. Our work now suggests that, although both kinases contribute to eIF4E phosphorylation and support PDAC cell proliferation under basal conditions, only MNK2

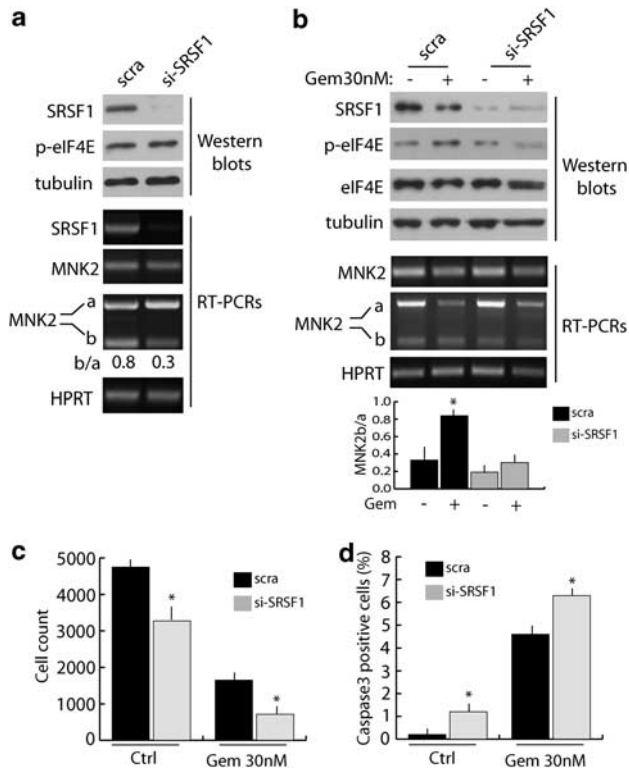


Figure 6. SRSF1 is required for the modulation of *MNKK2* splice variants by gemcitabine. **(a)** MiaPaCa2 cells transiently transfected with scrambled or SRSF1 siRNAs and analyzed after 48 h. Western blot analysis (first to third panel) of SRSF1, p-eIF4E and tubulin. RT-PCR analysis (fourth to seventh panel) of SRSF1, MNK2 total and splice variant mRNA levels (ratio quantified as in Figure 5). **(b)** MiaPaCa2 cells were transfected with control or SRSF1 siRNAs and treated with 30 nM gemcitabine for additional 48 h. Western blot analysis (first to fourth panel) of SRSF1, eIF4E, p-eIF4E and tubulin. RT-PCR analysis (fifth to seventh panel) of MNK2 and MNK2 splice variant mRNA levels as in **(a)**. * $P < 0.05$ in paired *t*-test. **(c, d)** MiaPaCa2 cells were transfected with scramble or SRSF1 siRNAs and treated with 30 nM gemcitabine for 48 h. The histogram in **(c)** represents cell number of three experiments (mean \pm s.d.). The histogram in **(d)** represents the percentage of cleaved-caspase3-positive cells of three experiments (mean \pm s.d.). Statistical analysis was performed comparing values of cells silenced for SRSF1 with cells transfected with the control siRNA; * $P < 0.05$ in paired *t*-test.

is responsible for the pro-survival effects in cells treated with gemcitabine. Thus, our results uncover a new MNK2-specific function in PDAC cells, which confers resistance to a genotoxic treatment. As MNK2 was found to be upregulated in hormone-resistant prostate cancer,¹² it will be interesting to test whether it is more generally involved in the pro-survival responses of cells that develop resistance to chemotherapeutic treatments.

The *MNKK2* gene encodes two mRNA variants, through usage of alternative last exons named 13a (MNK2a) and 13b (MNK2b).^{9,20} Gemcitabine caused a reduction in MNK2 expression, mainly affecting MNK2a levels and thereby altering the splice variant ratio in favor of MNK2b. We also found that MNK2b partially protected cells from gemcitabine-induced apoptosis, whereas MNK2a did not. MNK2b lacks the MAPK-interacting region and it is thereby uncoupled from upstream MAPK pathways.^{9,20,21} Thus, it is possible that its expression in cells treated with gemcitabine allows higher levels of eIF4E phosphorylation independently from external cues, which might lead to progressive selection of chemoresistant cells. Splicing of MNK2b was previously shown to be regulated by the splicing factor SRSF1 in other cell types.²¹

We found that gemcitabine induces the expression of SRSF1 in PDAC cells, which is necessary to favor MNK2b splicing under genotoxic stress. In the absence of SRSF1, gemcitabine still caused a reduction in MNK2 levels, but it did not alter the ratio between the two splice variants, indicating that SRSF1 is required to promote MNK2b splicing in PDAC cells exposed to the drug. Moreover, SRSF1 silencing impaired eIF4E phosphorylation and reduced viability of PDAC cells exposed to gemcitabine. These observations suggest that SRSF1 upregulation is part of the pro-survival response triggered by gemcitabine. Interestingly, *SRSF1* is an oncogene frequently upregulated in cancer.²¹ More in general, splicing factors are emerging as novel regulators of oncogenic transformation, and increased expression of some of them was shown to correlate with malignancy and poor prognosis.²² Furthermore, mutations that affect splicing of tumor suppressors, such as BRCA1/2 and APC, resulting in their inactivation, account for some types of inherited and sporadic susceptibility to cancer.^{26,27} Our results now suggest that increased expression of splicing factors and changes in alternative splicing of target genes can also occur in response to chemotherapeutic treatment of cancer cells. Thus, targeting the activity of splicing factors might represent a novel approach for combined treatments of specific cancers. In this regard, it is noteworthy that the SR protein kinase 1, a key regulator of SRSF1 activity, is also upregulated in PDAC²⁸ and was proposed as a suitable target for novel therapies.²⁹

In conclusion, our study identifies a novel pro-survival pathway triggered by gemcitabine in PDAC cells, which relies on MNK2-dependent phosphorylation of eIF4E, and suggests that targeting this pathway might represent a promising approach to enhance the response of PDAC cells to therapeutic agents.

MATERIALS AND METHODS

Tissue, histopathology and clinical information

Immunohistochemistry was performed with a rabbit polyclonal anti phospho-eIF4E antibody (1:200, Invitrogen, Rockville, MD, USA), as previously described,¹⁸ on paraffin-embedded tissue samples from 32 primary non metastatic PDAC patients receiving surgery with radical intent. All but eight of these patients received gemcitabine-based adjuvant therapy after surgery. None of the patients received neoadjuvant treatment. Clinical and histopathological data for each patient were recorded (Supplementary Table 1). Scoring of p-eIF4E was based on distribution and intensity of staining in neoplastic cells.¹⁸ Distribution was scored as 0 (0%), 1 (1–50%) and 2 (51–100%). Intensity was scored as 0 (no signal), 1 (mild), 2 (intermediate), 3 (strong) (Figure 1a). Values were summed in a total score from 0 to 5. Samples were classified as 'low p-eIF4E' expression when score was ≤ 2 (group 0), and as 'high p-eIF4E' expression when score was ≥ 3 (group 1). Statistical analysis was performed by MedCalc 9.6 (www.medcalc.be). Differences for continuous variables were evaluated by *t*-test and for categorical variables by Fisher's test. Correlation between the expression scores and pathological data was tested by Spearman's rank order correlation. Analysis of overall survival was performed by Kaplan–Meier method and analyzed by log-rank test. Patients lost at follow-up or whose follow-up ended before the outcome (death) was reached, are 'censored' and marked as small vertical lines in the survival curves. Univariate and multivariate analyses for risk factors affecting survival were performed by Cox-proportional hazards regression model test; a *P*-value < 0.05 was considered as statistically significant.

Cell cultures, treatments and extract preparation

MiaPaCa2, PT45P1 and PANC-1 cells were obtained from the Cancer Research UK Cell Services (Clare Hall Laboratories, Potters Bar, UK); HPAF2 cells were purchased from American Type Culture Collection (ATCC, Rockville, MD, USA) and generously provided by Professor Aldo Scarpa (University of Verona). Cells were maintained in Dulbecco's modified Eagle's medium (GIBCO, Carlsbad, CA, USA) (MiaPaCa2) or RPMI 1640 (Lonza, Basel, Switzerland) (PT45P1, PANC-1, HPAF2) supplemented with 10% fetal bovine serum. MNK-Inhibitor (CGP57380), rapamycin, LY294002, U0126 and SB202190 (EMD Chemical Inc./Calbiochem, Darmstadt,

Germany) were dissolved in dimethyl sulfoxide and stored at -20°C . Gemcitabine (Eli Lilly & Company, Indianapolis, IN, USA) was dissolved in water. Cisplatin (Sigma-Aldrich, St Louis, MO, USA) was dissolved in RPMI 1640. Stock solutions were diluted to the final concentrations in medium. After incubation, cells were washed with ice-cold phosphate buffered saline (PBS), resuspended in lysis buffer (100 mM NaCl, 15 mM MgCl_2 , 30 mM Tris-HCl pH 7.5, 1 mM dithiothreitol, 2 mM Na-orthovanadate, 1% Triton X-100 and Protease-Inhibitor Cocktail (Sigma-Aldrich)) and kept on ice for 10 min. Cell extracts were separated by centrifugation at 12 000 r.p.m. for 10 min and diluted in SDS-PAGE sample buffer.

SDS-PAGE and western blot analyses

Western blot analyses of cell extracts (30 μg) were performed as previously described^{11,30} using the following primary antibody: mouse anti beta tubulin (1:1000, Sigma-Aldrich); rabbit anti-4EBP1, anti-rpS6 and anti-eIF4E (1:1000, Cell Signaling Technology, Danvers, MA, USA); rabbit anti-p-rpS6 and anti-p-eIF4E (1:1000, Biosource, Carlsbad, CA, USA); mouse anti-SRSF1 and anti-hnRNP1, rabbit anti-Sam68 and anti-ERK2 (1:1000, SantaCruz Biotechnology, Santa Cruz, CA, USA). Secondary IgGs conjugated with horseradish peroxidase (1:10 000; Amersham Bioscience, Piscataway, NJ, USA) were incubated for 1 h at room temperature and signals were detected by enhanced chemiluminescence (SantaCruz Biotechnology).

Cell count and viability assays

MiaPaCa2 were seeded at 50 000 cells/plate in 24-well plate and treated as described in the text for 72 h, washed in PBS, trypsinized and counted using the Thoma's chamber. Cell viability was measured by the MTS Cell Titer 96 Aqueous Non-Radioactive Cell Proliferation Assay (Promega, Madison, WI, USA) according to manufacturer's instructions by plating 1500 cells (MiaPaCa2) or 3000 cells (PT45P1) per well. Results of cell count and cell viability assays represent mean \pm s.d. of three experiments performed in triplicate.

Colony formation assay

Single-cell suspensions were plated in 100 mm plates (3500 cells/plate). After 1 day, cells were treated for 24 h with gemcitabine (0.1 and 0.3 nM) and MNK-I (10 μM) alone or in combination. At the end of the incubation, the medium was replaced every 24 h with or without addition of 5 μM MNK-I. After 10 days, cells were fixed in methanol for 10 min, stained overnight with 10% Giemsa, washed twice in PBS and dried. Pictures were taken using a digital camera to count the colonies. Results represent the mean \pm s.d. of three experiments.

Immunofluorescence analysis

For eIF4E phosphorylation, MiaPaCa2 were seeded at 350 000 cells/plate in 35 mm dishes and treated with 30 nM gemcitabine with or without 10 μM MNK-I for 24 h. Cell lines were then fixed for 10 min in 4% paraformaldehyde (PFA), permeabilized with 0.1% Triton X-100, processed for immunofluorescence analysis using the anti p-eIF4E (1:200). For apoptotic markers, cells were seeded at 250 000 (MiaPaCa2, HPAF2) or 200 000 (PT45P1) cells/plate in 35 mm plates and treated with gemcitabine for 72 or 48 h. Immunofluorescence was performed as described above and cell were stained with anti-cleaved caspase-3 antibody (1:500; Sigma-Aldrich). For TUNEL assays, fixed cells were permeabilized in PBS containing 0.1% sodium citrate and 0.1% Triton X-100 and incubated with TUNEL reaction mixture containing terminal deoxynucleotidyltransferase and fluorescein-dUTPs at 37°C for 60 min (In Situ Cell Death Detection Kit, Fluorescein, Roche, Penzberg, Germany). Four random fields were chosen for each treatment and at least 100 cells/field were counted. Results represent the mean \pm s.d. of three experiments.

Cell transfection experiments

pEGFP MNK2a and pEGFP MNK2b vectors were obtained by subcloning the *EcoRI/Sall* (MNK2a, 2b) fragments from pEBG (MNK2a) or pCMV5 (MNK2b) (generous gift of Dr CG Proud) in pEGFP1 vector. MiaPaCa2 cells were transfected in 35 mm plates with 2 μg of plasmid using Lipofectamine 2000 (Invitrogen) by standard methods as described.^{30,31}

MNK1 silencing was obtained using the Smart pool reagent mix from Dharmacon. MNK2 si-RNA 5'-GGAACGUCCUAGAGCUGAU-3' (common to both splice variants of the gene) and SRSF1 si-RNA 5'-CCAAGGACAUU GAGGACGU-3' were purchased from Sigma-Aldrich. Cells were transfected

at 50% confluence in 35 mm plates with 30 nM of siRNAs using Lipofectamine RNAi MAX reagent (Invitrogen).³¹

RT-PCR analyses

RNA was extracted using the TRIzol reagent (Invitrogen) and following manufacturer's instruction. After digestion with RNase-free DNase (Roche Diagnostics GmbH), 1 μg of RNA was retro-transcribed (RT) using M-MLV reverse transcriptase (Invitrogen). PCR primers for MNK1 and MNK2 splice variants and PCR conditions were previously described.^{21,32} For MNK1 and MNK2 expression we used primers that amplify both splice variants: MNK1 forward 5'-GAGGTTCCATCTTAGCCACAT-3', reverse 5'-ACGATGAGCAAT GCCTTTGGT-3'; MNK2 forward 5'-CGCCTTGGACTTTCTGCATAA-3', reverse 5'-TCACAGATCTTACGGGGGA-3'. For *SRSF1* expression, the following primers were used: forward 5'-ATGTCGGGAGGTGGTGTGATTCGT-3', reverse 5'-TTATGT ACGAGAGCGAGATCTGCT-3'. Ten percent of the RT reaction was used for each PCR reaction.

CONFLICT OF INTEREST

The authors declare no conflict of interest.

ACKNOWLEDGEMENTS

We wish to thank Professor CG Proud for the generous gift of MNK2a and MNK2b plasmids, Professor A Scarpa for the gift of HPAF2 cells, Dr Enrica Bianchi for help with FACS analysis, Dr Maria Antonietta Talerico for technical support with immunohistochemistry and Dr Alessia Di Florio for helpful suggestions throughout the study. This work was supported by funds from the Associazione Italiana Ricerca sul Cancro (AIRC IG10348) and Association for International Cancer Research (AICR).

REFERENCES

- Kern SE, Shi C, Hruban RH. The complexity of pancreatic ductal cancers and multidimensional strategies for therapeutic targeting. *J Pathol* 2011; **223**: 295–306.
- Falasca M, Selvaggi F, Buus R, Sulpizio S, Edling CE. Targeting phosphoinositide 3-kinase pathways in pancreatic cancer—from molecular signaling to clinical trials. *Anticancer Agents Med Chem* 2011; **11**: 455–463.
- Sun SY, Rosenberg LM, Wang X, Zhou Z, Yue P, Fu H *et al*. Activation of Akt and eIF4E survival pathways by rapamycin mediated mammalian target of rapamycin inhibition. *Cancer Res* 2005; **65**: 7052–7058.
- Wang X, Yue P, Chan C, Ye K, Ueda T, Watanabe-Fukunaga R *et al*. Inhibition of Mammalian Target of Rapamycin Induces Phosphatidylinositol 3-Kinase Dependent and Mnk-Mediated Eukaryotic Translation Initiation Factor 4E Phosphorylation. *Mol Cell Biol* 2007; **27**: 7405–7413.
- Zoncu R, Efeyan A, Sabatini DM. mTOR: from growth signal integration to cancer, diabetes and ageing. *Nat Rev Mol Cell Biol* 2011; **12**: 21–35.
- Culjkovic B, Topisirovic I, Skrabanek L, Ruiz-Gutierrez M, Borden KL. eIF4E promotes nuclear export of cyclin D1 mRNAs via an element in the 3' UTR. *J Cell Biol* 2005; **169**: 245–256.
- Mamane Y, Petroulakis E, Rong L, Yoshida K, Ler LW, Sonenberg N. eIF4E – from translation to transformation. *Oncogene* 2004; **23**: 3172–3179.
- Ueda T, Watanabe-Fukunaga R, Fukuyama H, Fukuyama H, Nagata S, Fukunaga R. Mnk2 and Mnk1 are essential for constitutive and inducible phosphorylation of eukaryotic initiation factor 4E but not for cell growth or development. *Mol Cell Biol* 2004; **24**: 6539–6654.
- Buxade M, Parra-Palau JL, Proud CG. The Mnk: MAP kinase-interacting kinases (MAP kinase signal-integrating kinases). *Front Biosci* 2008; **13**: 5359–5373.
- Zhang Y, Li Y, Yang D. Phosphorylation of eIF-4E positively regulates formation of the eIF-4F translation initiation complex following DNA damage. *Biochem Biophys Res Commun* 2008; **367**: 54–59.
- Bianchini A, Loiarro M, Bielli P, Busà R, Paronetto MP, Loreni F *et al*. Phosphorylation of eIF4E supports protein synthesis, cell cycle progression and proliferation in prostate cancer cells. *Carcinogenesis* 2008; **29**: 2279–2288.
- Konicek BW, Stephens JR, McNulty AM, Robichaud N, Peery RB, Dumstorf CA *et al*. Therapeutic inhibition of MAP kinase interacting kinase blocks eukaryotic initiation factor 4E phosphorylation and suppresses outgrowth of experimental lung metastases. *Cancer Res* 2011; **71**: 1849–1857.
- Altman JK, Glaser H, Sassano A, Joshi S, Ueda T, Watanabe-Fukunaga R *et al*. Negative Regulatory Effects of Mnk Kinases in the Generation of Chemotherapy-Induced Antileukemic Responses. *Mol Pharmacol* 2010; **78**: 778–784.
- Wendel HG, Silva RL, Malina A, Mills JR, Zhu H, Ueda T *et al*. Dissecting eIF4E action in tumorigenesis. *Genes Dev* 2007; **21**: 3232–3237.

- 15 Furic L, Rong L, Larsson O, Koumakpayi IH, Yoshida K, Brueschke A *et al*. eIF4E phosphorylation promotes tumorigenesis and is associated with prostate cancer progression. *Proc Natl Acad Sci USA* 2010; **107**: 14134–14139.
- 16 Ueda T, Sasaki M, Elia AJ, Chio II, Hamada K, Fukunaga R *et al*. Combined deficiency for MAP kinase-interacting kinase 1 and 2 (Mnk1 and Mnk2) delays tumor development. *Proc Natl Acad Sci USA* 2010; **107**: 13984–13990.
- 17 Graff JR, Konicek BW, Lynch RL, Dumstorf CA, Dowless MS, McNulty AM *et al*. eIF4E activation is commonly elevated in advanced human prostate cancers and significantly related to reduced patient survival. *Cancer Res* 2009; **69**: 3866–3873.
- 18 Yoshizawa A, Fukuoka J, Shimizu S, Shilo K, Franks TJ, Hewitt SM *et al*. Overexpression of phospho-eIF4E is associated with survival through AKT pathway in non-small-cell lung cancer. *Clin Cancer Res* 2010; **16**: 240–248.
- 19 Chrestensen CA, Eschenroeder A, Ross WG, Ueda T, Watanabe-Fukunaga R, Fukunaga R *et al*. Loss of MNK function sensitizes fibroblasts to serum-withdrawal induced apoptosis. *Genes Cells* 2007; **12**: 1133–1140.
- 20 Scheper GC, Parra JL, Wilson M, Van Kollenburg B, Vertegaal AC, Han ZG *et al*. The N and C termini of the splice variants of the human mitogen-activated protein kinase-interacting kinase Mnk2 determine activity and localization. *Mol Cell Biol* 2003; **23**: 5692–5705.
- 21 Karni R, De Stanchina E, Lowe SW, Sinha R, Mu D, Krainer AR. The gene encoding the splicing factor SF2/ASF is a proto-oncogene. *Nat Struct Mol Biol* 2007; **14**: 185–193.
- 22 David CJ, Chen M, Assanah M, Canoll P, Manley JL. HnRNP proteins controlled by c-Myc deregulate pyruvate kinase mRNA splicing in cancer. *Nature* 2010; **463**: 364–368.
- 23 Bielli P, Busà R, Paronetto MP, Sette C. The RNA-binding protein Sam68 is a multifunctional player in human cancer. *Endocr Relat Cancer* 2011; **18**: 91–102.
- 24 Assouline S, Culjkovic B, Cocolakis E, Rousseau C, Beslu N, Amri A *et al*. Molecular targeting of the oncogene eIF4E in AML: a proof-of-principle clinical trial with ribavirin. *Blood* 2009; **114**: 257–260.
- 25 Wolpin BM, Hezel AF, Abrams T, Blaszczak LS, Meyerhardt JA, Chan JA *et al*. Oral mTOR inhibitor everolimus in patients with gemcitabine-refractory metastatic pancreatic cancer. *J Clin Oncol* 2008; **27**: 193–198.
- 26 Gonçalves V, Theisen P, Antunes O, Medeira A, Ramos JS, Jordan P *et al*. A missense mutation in the APC tumor suppressor gene disrupts an ASF/SF2 splicing enhancer motif and causes pathogenic skipping of exon 14. *Mutat Res* 2009; **662**: 33–36.
- 27 Sanz DJ, Acedo A, Infante M, Durán M, Pérez-Cabornero L, Esteban-Cardeñosa E *et al*. A high proportion of DNA variants of BRCA1 and BRCA2 is associated with aberrant splicing in breast/ovarian cancer patients. *Clin Cancer Res* 2010; **16**: 1957–1967.
- 28 Hayes GM, Carrigan PE, Miller LJ. Serine-arginine protein kinase 1 overexpression is associated with tumorigenic imbalance in mitogen-activated protein kinase pathways in breast, colonic, and pancreatic carcinomas. *Cancer Res* 2007; **67**: 2072–2080.
- 29 Hayes GM, Carrigan PE, Beck AM, Miller LJ. Targeting the RNA splicing machinery as a novel treatment strategy for pancreatic carcinoma. *Cancer Res* 2006; **66**: 3819–3827.
- 30 Busà R, Paronetto MP, Farini D, Pierantozzi E, Botti F, Angelini DF *et al*. The RNA-binding protein Sam68 contributes to proliferation and survival of human prostate cancer cells. *Oncogene* 2007; **26**: 4372–4382.
- 31 Pedrotti S, Bielli P, Paronetto MP, Ciccocanti F, Fimia GM, Stamm S *et al*. The splicing regulator Sam68 binds to a novel exonic splicing silencer and functions in SMN2 alternative splicing in spinal muscular atrophy. *EMBO J* 2010; **29**: 1235–1247.
- 32 O'Loughlen A, Gonzalez VM, Pineiro D, Pérez-Morgado MI, Salinas M, Martín ME. Identification and molecular characterization of Mnk1b, a splice variant of human MAP kinase-interacting kinase Mnk1. *Experimental Cell Res* 2004; **299**: 343–355.

Supplementary Information accompanies the paper on the Oncogene website (<http://www.nature.com/onc>)